AIAA JOURNAL
Vol. 41, No. 1, January 2003

Structural Integrity Redesign Through Neural-Network Inverse Mapping

R. M. Pidaparti,* S. Jayanti,† M. J. Palakal,‡ and S. Mukhopadhyay§
Indiana University—Purdue University at Indianapolis, Indianapolis, Indiana 46202

A neural-network inverse mapping approach was used in a structural integrity redesign problem to achieve the desired strength, corrosion, and fatigue properties. Also, through the inverse-mapping procedure the relative importance of damage parameters was obtained for two trained neural-network models. The damage parameters corresponding to a given strength and corrosion rate are predicted in one network, whereas the damage parameters corresponding to a given corrosion fatigue life are predicted in the other network. The results obtained from the inverse mapping procedure are compared with actual panel configurations and environments and experimental data. The results obtained through the inverse-mapping procedure are found to agree well with the experimental data, thus demonstrating the feasibility of the approach for the structural integrity redesign of aging aircraft structures.

I. Introduction

THE strength and durability of aging aircraft structures depend on various parameters like loading spectrum, material, geometry, and environment. Changes in the structural durability of aircraft structures might affect the performance to such an extent that remedial measures might become necessary. To reduce the repair and maintenance costs, one might perform early repair on the structures before the damage grows to a dangerous size. Alternatively, the repair might even be postponed until the aircraft is taken out of service for scheduled maintenance. In the latter case it might become important to adapt operational usage to limit or even stop the damage growth. If sufficient knowledge exists to relate damage rates to mission types, this can be achieved by conditioning monitoring.[1] Maintenance and repair of the structure will be easier if it is possible to obtain the maximum allowable values of the damage parameters so that the structural health of the aircraft does not adversely affect performance.

Consider a problem where an aircraft panel/structure is to be redesigned or repaired to achieve a particular reliability (strength, corrosion, or fatigue characteristics). In the normal design of such structures, only the structural failure mechanisms such as yielding, buckling, fracture, etc. are considered. However, the redesign of the structure should also take into account other damage mechanisms such as multiple-site damage (MSD), corrosion fatigue, and creep fatigue that will affect the durability of the structure. Therefore, the possibility of integrating structural design and selection of operating environment parameters with damage prediction for structural redesign is explored in this paper. This concept can also be used for stipulating flight requirements to aging aircraft.

Two neural-network (NN) models were developed to approximate the damage MSD and corrosion and corrosion-fatigue mechanisms in Refs. 2 and 3. The different damage parameters affecting the structural integrity can act together in different combinations to give a desired damage characteristic. For instance, an aircraft panel might have a large lead crack and a small MSD crack size but still have the same strength as a panel with considerably smaller lead crack and a slightly larger MSD crack at the rivet holes. However, because the NN is trained by updating the weights according to the importance of an input node for the output (strength, corrosion rating, or fatigue life) we can use the weights of the network as a means for obtaining the critical damage (input) parameters. The networks would produce sets of input parameters that correspond approximately to a given set of desired reliability properties. This might help in better understanding the interaction between the input parameters (geometric, fatigue, and environmental parameters of the panel) and the outputs (reliability properties) of the NN model.

To fulfill the objective of achieving the damage parameters corresponding to a particular desired reliability, we explore the method of inverse mapping that will utilize the knowledge stored in the trained NNs. In this study we have gone a step further and tried to predict the relevance of the damage parameters in the damage process by using the knowledge stored in the NNs. We rank order the damage parameters according to their relative importance in the damage mechanism by using the sensitivity of the outputs caused by the changes in inputs through NN inverse mapping. The inverse-mapping procedure was investigated for two NNs that capture the residual strength for MSD panels and corrosion-fatigue life of aircraft materials.

II. Inverse-Mapping Procedure

The procedure of inverse mapping using NNs has been used to solve engineering problems in various fields. For example, in remote sensing the geophysical parameters are obtained from measurements made by sensors,[4] using iterative inversion of NNs. In robotics the inverse kinematics problem, with the objective of computing the positions of joints that yield a given location for the arm, is solved using inverse mapping with NNs.[5,6]

The inverse-mapping methodology is a procedure to obtain the values of the input parameters that correspond to a particular desired value of the output(s). Figure 1 shows a flowchart of the inverse-mapping algorithm. The algorithm starts by predicting the outputs O_i from the NN model for a random input vector and compares the outputs with the desired values T_i provided to the algorithm. Subsequently, the error, if any, between the predicted and desired outputs is backpropagated through the network layers to the input layer. Each of the inputs is then adjusted according to the error that the input node receives and the weight associated with the connecting link. This process of predicting the output and updating the inputs is done iteratively, until the NN model has achieved the set of desired outputs with reasonable accuracy. This is similar to the gradient descent method used in the forward training of the NN, except that gradient descent is applied to the inputs rather than the weights of the NN. The inputs of the network can be adjusted using the following equation:

Received 14 August 2001; revision received 10 April 2002; accepted for publication 29 April 2002.

*Professor, Department of Mechanical Engineering, Purdue School of Engineering and Technology. Associate Fellow AIAA.
†Graduate Student, Department of Mechanical Engineering, Purdue School of Engineering and Technology. Member AIAA.
‡Professor and Chair, Department of Computer and Information Science, Purdue School of Science.
§Associate Professor, Department of Computer and Information Science, Purdue School of Science.

$$X(k+1) = X(k) - \eta \frac{\partial J}{\partial X} = X(k) - \eta \sum_{i=1}^{n_0} e_i \frac{\partial e_i}{\partial X} \tag{1}$$

$$J = \frac{1}{2}\sum e_i^2 = \frac{1}{2}\left(e_1^2 + e_2^2 + e_3^2 + \cdots + e_{n_o}^2\right) \tag{2}$$

where n_o is the number of outputs, e_i is the error at the ith output, η is the network learning rate, $X(k)$ represents the adjusted input after the kth iteration, and $X(k+1)$ represents the new input after $(k+1)$ iterations.

This equation is similar to that used for adjusting the weights in neural networks. However, the error is differentiated with respect to the inputs instead of the weights. Expressing this statement in terms of changes in the NN algorithm means that the backpropagation of error is done through one additional layer, namely, the input layer, thereby changing the values of the inputs.

Figure 2 shows the schematic description of the NN inverse mapping. While performing backpropagation of the error, the weights of the trained network are not changed because the trained weights are assumed to represent a sufficiently accurate functional relationship between the inputs and outputs. Hence, the effectiveness of this approach is contingent upon the proper training of the forward network for prediction.

The problem of inverse mapping is similar to regular optimization techniques, except that, rather than the output itself, the objective function in inverse mapping is the error J between the desired and predicted output, which is minimized by the gradient descent method by changing the input vector. In most engineering problems the optimization techniques used are constrained optimization techniques because many solutions obtained from unconstrained optimization might not be feasible. The same argument is true for inverse-mapping techniques in engineering as well. In the present study care has been taken while writing the computer code to constrain the input space during inverse mapping so as to get feasible damage parameters. However, unlike many optimization techniques there is no penalty associated with the constraints. Instead, the value of a particular input remains unchanged once it reaches the boundary of the feasible space. Different combinations of input parameters can produce the same output values. We choose to keep certain inputs steady while varying the other inputs to obtain the different combinations. Given a desired output value, it is possible to obtain the values of a few inputs, while the values of the rest are provided to the network. This might correspond with the situation where some of the damage parameters cannot be changed for a given structure. For example, an aluminum panel, present as part of an operational aircraft structure, will already have rivet holes, and the diameter and spacing of the holes cannot be changed while redesigning. The computer code developed in this study for inverse mapping can be also used to obtain the input parameters for desired value(s) of a single or multiple output parameters.

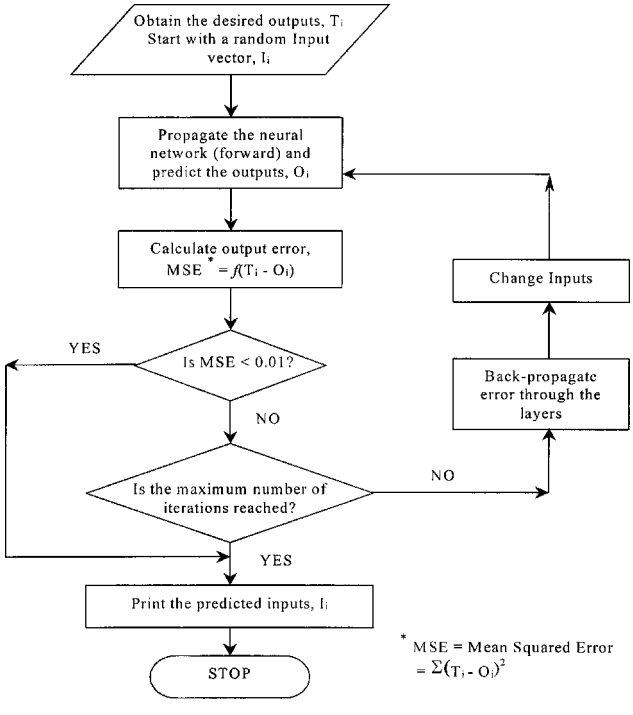

Fig. 1 Flowchart of the inverse-mapping algorithm.

III. Relative Importance of Operating Parameters

Several operating parameters affect the structural durability of an aging aircraft structure. Hence it is important to understand which parameters are more important, thereby emphasizing those parameters in predicting structural integrity. Specifically, the goal of this study is to obtain the relative importance of the damage parameters related to the operating environment for a given damage mechanism. This will help identify the damage parameter most critical to the structure's integrity. The relative importance of parameters is achieved through the backpropagating algorithm in the NN method.

While backpropagating the error from the output to the input in the inverse-mapping approach (Fig. 1), the input update takes place by using the derivative of the output mean-square error E with respect to the input I_k as shown in Eq. (3). However, the output error is a function of the output and the target:

$$I_k \leftarrow I_k + \eta \frac{\partial E}{\partial I_k} = I_i + \eta a_j e_i \frac{\partial g(in_i)}{\partial I_k} \tag{3}$$

In this study we use the backpropagating algorithm to obtain the derivative of the outputs O_i with respect to the inputs I_k. In particular, the output is also backpropagated, in addition to the error, and is differentiated with respect to the input. This quantity $(\partial O_i/\partial I_k)$ is the gradient of the output with respect to the particular input. We average this derivative over the whole training set, which represents the typical input space for the problem. As the training error converges, so do the derivatives, thereby giving the converged average values of the derivatives over the entire input space. We will then have a matrix of averaged derivatives of the order $n_o \times n_i$, where n_o and n_i are the number of outputs and inputs, respectively. If the value of the average derivative for a particular input is very small compared

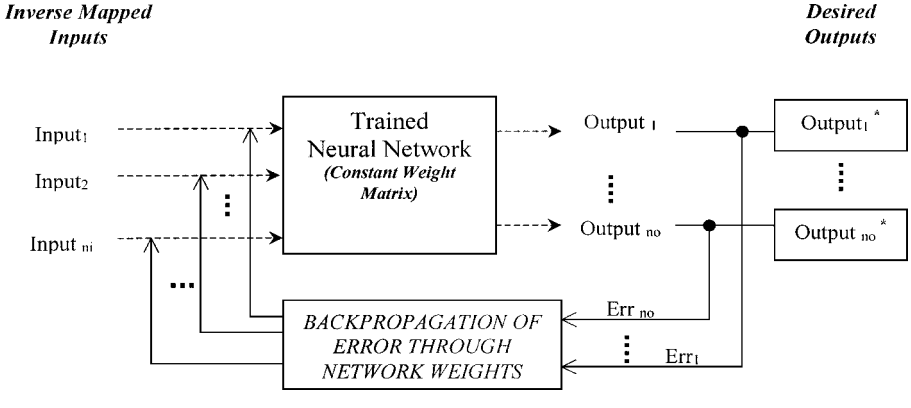

Fig. 2 Schematic of inverse-mapping network.

to those for the rest, it can be safely assumed that the particular input is less important in the input space considered. This is easily inferred because a smaller value of the derivative implies that the change in the input has a small effect on the output. It was observed that the relative final values of these derviatives, after nearly 10,000 epochs, were similar to those in the middle of training (around 1000 epochs). If in the middle of training the derivative was smallest for a particular input, the derivative remained smallest for the same input in the last epoch as well. Thus, after a few iterations the network is able to ascertain the relative importance of the input parameters. This simple methodology worked well in determining the importance of the network inputs (damage parameters). However, for the importance prediction by this method to be valid for a large input space, training examples might need to be provided for a similar input space.

IV. Results and Discussion

The inverse-mapping procedure and the relative importance of parameters affecting a particular damage mechanism are applied to two trained networks. One is residual strength and corrosion rate network (NN I), and the other is the corrosion-fatigue network (NN II). The details of these forward networks model can be found in Refs. 2 and 3. Both the developed neural network models (NN I and II) have successfully captured the underlying physical relationships in various damage mechanisms and are used in the current study for redesign of the aircraft structures. The results pertaining to structural redesign for these two networks are described next.

Redesign for Residual Strength and Corrosion Rate

The parameters affecting only the residual strength of the panel are panel width, number of holes, hole diameter, center crack length, average MSD crack length, and material lost, whereas those affecting the corrosion rate and corrosion rating of the panel include the material type, corrosion environment type, yield strength, temperature, and the duration of exposure. Yield strength and panel thickness are the two inputs that are common to both these phenomena. After developing the neural network model (NN I) for predicting the residual strength and corrosion rates,[2] inverse mapping was performed on the network, and the values of the damage parameters were obtained for desired strength and corrosion rates. The inverse-mapping network converged to within 2% of the desired strength and corrosion values, in fewer than 100,000 iterations, for all of the test cases considered. To validate the present method of inverse mapping, a few simulations were carried out and compared with available experimental data. The damage parameters obtained from inverse mapping for most of the panels were quite close to those of the experimental values. Because of the large number of damage parameters in the NN I model, the problem of inverse mapping could have many solutions (that is, different combinations of damage parameters can result in the same strength or corrosion rate in the panel). Therefore, we constrained certain damage parameters in the network and predicted the rest of the damage parameters.

A set of eight panels was used to test the damage parameter prediction for desired residual strength. Table 1 presents the results for these cases. For all of the panels, the residual strengths were close to the desired values. However, the damage parameters were different from the experimental values for a few panels. For the Boeing[7] panel B7-3 the thickness mapped by the network is nearly the same as that of the test panel with the rest of the input parameters being the same. For cases 1–4 in Table 1 where a single input is mapped, although the rest of the panel configurations are kept the same the inputs predicted are within 10% of the experimental data. For case 5 (RS-05b panel[8]), however, for the same strength the lead crack size predicted by the network is 17% less, whereas the pitch of the rivet holes is 9.7% higher than the experimental data. For case 6 (RS-05b panel[8]) smaller lead crack and larger MSD crack give almost the same strength as the experimental strength, which is feasible in reality, although there might be a reduction in strength depending on the magnitudes of the crack lengths. The MSD crack length used in this study is the average MSD crack length, which is assumed to be the same for all of the holes that have an MSD crack. A panel with smaller rivet holes will have a larger net section and hence a higher load-carrying capacity; however, a larger lead crack reduces the cross-sectional area and thereby the strength of the panel. This effect is clearly seen in case 7, where the panel configuration predicted by the inverse-mapping algorithm has the same strength as the experiments but has a smaller diameter hole and a larger lead crack. In case 8 the inverse-mapping model was allowed to search, simultaneously, through the feasible space for three input parameters, while the rest of the damage parameters were held constant. The model predicts the panel will have the same strength for smaller MSD crack length, larger lead crack length, and a smaller rivet hole diameter.

Two test cases were studied for the corrosion rate and the American Society for Testing and Materials (ASTM) G34 rating of the MSD panels. Table 2 shows the results obtained for both the cases. It can be seen from Table 2 that the damage parameters predicted

Table 2 Predictions of inverse mapping for desired corrosion rate of 0.075 cm^2/cm-days and ASTM G34 corrosion rating of 0.4

Case	Experimental value	Predicted input	Experimental value	Predicted input
	Yield strength, MPa		*Thickness, mm*	
1	454.5	454.5	2.250	2.286
	Temperature, °C		*Duration of exposure, days*	
2	29.50	29.24	1825	1758

Table 1 Predictions of inverse mapping for desired residual strength

Case	Panel ID (reference)	Desired residual strength	Predicted residual strength	Input parameter					
				Expt. data	Predicted	Expt. data	Predicted	Expt. data	Predicted
				Thickness of panel					
1	B7-3 (7)	97.32	97.20	0.158	0.162	——		——	
				Yield strength					
2	RS-05b (8)	348.79	341.81	374.39	387.69	——		——	
				Lead crack					
3	RS-05b (8)	348.79	343.73	4.763	5.122	——		——	
				%Material remaining					
4	RS-05b (8)	348.79	340.77	100	99.9	——		——	
				Hole pitch		*Lead crack*			
5	RS-05b (8)	348.79	344.67	1.905	2.090	4.763	4.043	——	
				MSD crack length		*Lead crack*			
6	RS-05b (8)	348.79	340.30	0	0.126	4.763	3.309	——	
				Diameter		*Lead crack*			
7	RS-05a (8)	345.81	344.60	1.620	1.020	3.640	4.520	——	
				Diameter		*Lead crack*		*MSD crack*	
8	RS-04a (8)	267.34	267.17	1.514	1.179	4.675	6.414	0.279	0.252

by the inverse-mapping procedure are in good agreement with the experimental data. For case 1 the NN predicts the thickness higher than the experimental data, but the corrosion rate is lower than the experiments. Corrosion rate is the thickness lost per unit surface area per day of exposure. Hence, the greater the thickness of the panel, the lower the corrosion rate. For case 2 the inverse-mapping predictions for the duration of exposure and temperature are almost similar to those in the experiments for the same values of corrosion rate and ASTM G34 rating.

Relative Importance of Parameters for Residual Strength and Corrosion Rate

Table 3 provides the relative importance of the various inputs in terms of percentage and ranks obtained using the approach just discussed. It can be observed that for residual strength the top five most important parameters are the center (lead) crack length, postcorrosion material, MSD crack length yield strength, and the pitch of the rivet holes (hole spacing). The results also illustrate the fact that the presence of MSD along with the lead crack can significantly affect the residual strength of the panel. In fact, the relative importance percentages indicate that the MSD crack has almost the same importance (13.31%) as compared to the center (lead) crack (14.38%). Hence, both of these parameters are equally detrimental to the residual strength of the structure.

Similarly, for the corrosion rate in the panel the duration of exposure was the most important parameter. The second most important parameter is the yield strength, which can indirectly be representative of the exact chemical composition of the aluminum alloy. The resistance to corrosion is affected by the presence of metals like copper, magnesium, etc. in the aluminum alloy. The third most important parameter is the type of corrosive environment that the aircraft is operating under. The fourth and fifth parameters predicted by the approach to be important are, however, not related to corrosion and hence cannot be justified as important, although they constitute a large percentage. Similarly, for ASTM G34 corrosion rating the postcorrosion material is shown as the most important parameter. However, this parameter was initially not deemed important in the model. The rest of the input parameters shown in the table for the corrosion rating are not directly related to the corrosion mechanism. Although discussed in Ref. 2, it can be reiterated here that the NN model for corrosion prediction needs to be further investigated for the discrepancies in the ASTM G34 corrosion rating prediction, and more data are also needed for reasonably training the NN.

Redesign for Corrosion Fatigue

The various parameters affecting the corrosion-fatigue mechanisms include maximum stress amplitude $\Delta\sigma$, stress ratio R, frequency of loading f, and duration of exposure D_{exp} of the material to corrosive environment. Corrosion-fatigue crack growth rates are strongly influenced not only by the specific combinations of cyclic loads, material, and environment, but also by the crack size. Hence, the critical pit size a_{ci}, the initial pit size a_0, and the final crack size a_f, before failure (as defined by the user or the inspection criteria), are also used as the inputs to the NN model developed.[3] The problem of predicting the damage parameters of a panel subjected to corrosion fatigue, so as to achieve desired values of the fatigue life, was investigated through inverse-mapping technique as discussed in Sec. II. Before using the inverse-mapping method for damage parameter prediction, the method needs to be validated against available experimental data. Table 4 presents the comparison between the predictions and the actual experiments for this problem. The values on the top of each row show the fatigue lives achieved by the inverse-mapping network (for example, for case 1, $N_i = 10{,}076$ and $N_p = 69{,}711$ cycles) and the corresponding damage parameter (for example, for case 1, $a_{\text{ci}} = 0.060$ mm) predictions. The values on the bottom of each column are the desired experimental values of lives and the corresponding damage parameter values from experiments.

For case 1 the desired crack initiation life (10,093 cycles), propagation (57,916 cycles) life, and the corresponding damage parameters ($a_{\text{ci}} = 0.074$ mm) from experimental data are presented in the table. In this case only the critical crack size (a_{ci}) is predicted (shown with an $*$), whereas the other parameters are already given to the network. In case 2 also, the critical pit size is predicted for the desired life cycles, whereas the rest of the damage parameters were provided to the network. Cases 3 and 4 predict the values of stress amplitude and the critical pit size. It can be observed that the network predicts lower stress amplitudes for both of the cases, but predicts a larger critical pit size (0.131 mm) for case 3 and a smaller critical pit size (0.059) for case 4, as compared to experimental data for the given fatigue lives, respectively.

Finally, in case 5 a total of three damage parameters were predicted simultaneously for fatigue life the same as case 3. The network predicts higher values for stress amplitude and duration of exposure to corrosion, but a smaller critical pit size as compared to experimental values for the same magnitudes of fatigue lives. An increase in the stress amplitude, keeping the stress ratio constant, has the effect of reducing the fatigue life of the material.[9] Increasing the duration of exposure also has the same effect. However, a

Table 3 Sensitivity studies of inputs for importance on the outputs for MSD mechanism

Rank	Effect on residual strength	Relative importance, %	Effect on corrosion rate	Relative importance, %	Effect on ASTM G34 corrosion rating	Relative importance, %
1	Lead crack length	14.38	Duration of exposure	27.38	Postcorrosion material	18.18
2	Postcorrosion material	13.36	Yield strength	14.64	Number of rivet holes	13.63
3	Average MSD crack length	13.31	Environment type	14.01	Lead crack length	13.63
4	Yield strength	12.88	Center crack length	14.01	Width	9.09
5	Hole spacing	8.97	Average MSD crack length	13.37	Hole spacing	9.09

Table 4 Comparison of damage parameter predictions by the inverse-mapping network with experimental data for corrosion fatigue

	Input parameter							Output parameter	
Cases	Stress amplitude $\Delta\sigma$, MPa	Duration of exposure D_{exp}, hr	Stress ratio	Frequency, cycles/day	Initial pit size a_0, mm	Critical crack pit depth a_{ci}, mm	Final crack size a_f, mm	Initiation life	Propagation life
1	233.96	71.97	−1	10.0	0.015	0.060[a]	10.0	10,076[b]	69,711[b]
Expt. data	233.96	71.97	−1	10.0	0.015	0.074	——	10,093	57,916
2	179.98	191.85	0.1	10.0	0.001	0.128[a]	3.0	32,004[b]	148,457[b]
Expt. data	179.98	191.85	0.1	10.0	0.001	0.128	——	33,806	148,457
3	176.14[a]	191.99	0.1	10.0	0.001	0.131[a]	3.0	33,806[b]	148,457[b]
Expt. data	179.98	191.99	0.1	10.0	0.001	0.128	——	33,806	148,457
4	218.67[a]	207.98[a]	0.1	10.0	0.001	0.096[a]	3.0	33,806[b]	148,457[b]
Expt. data	179.98	191.99	0.1	10.0	0.001	0.128	——	33,806	148,457
5	177.00[a]	191.99	0.1	10.0	0.001	0.059[a]	3.0	20,946[b]	400,682[b]
Expt. data	179.98	191.99	0.1	10.0	0.001	0.099	——	20,946	398,107

[a]Damage parameters predicted by the NN II (rest of the parameters being same as experiments). [b]Fatigue life values predicted by NN II.

Table 5 Simulations for maximizing/minimizing the initiation and propagation lives

No.	Case	Stress amplitude $\Delta\sigma$, MPa	Duration of exposure $D_{\exp}$, hr	Stress ratio	Frequency, cycles/day	Initial pit size a_0, mm	Critical crack pit depth a_{ci}, mm	Final crack size a_f, mm	Initiation life	Propagation life
1	Maximum N_p	198.9	124.92	0.32	6.86	$9.00E-02$	0.055	4.3	1	391,742
2	Maximum N_i	504.5	302.40	−0.62	11.50	$1.99E-02$	0.631	2.0	163,268	168
3	Minimum N_i and N_p	504.5	7.79	−0.98	1.54	$6.18E-02$	0.995	1.2	4	73
4	Maximum N_i	504.5	335.66	−0.60	17.20	$1.90E-02$	0.955	2.0	1,373,485	204
5	Maximum N_i and N_p	0.2	335.66	−0.98	3.82	$5.02E-04$	0.059	9.9	1,950,743	1,637,759

Table 6 Sensitivity studies of inputs for importance on outputs for corrosion-fatigue damage mechanism

Rank	Effect on initiation life	Relative importance, %	Effect on propagation life	Relative importance, %
1	Duration of exposure	26.75	Critical pit size	34.59
2	Stress amplitude	21.06	Stress ratio	25.58
3	Stress ratio	15.31	Duration of exposure	15.48
4	Initial pit size	14.50	Final crack size	11.43
5	Critical pit size	13.97	Stress amplitude	7.42

smaller critical pit size means a smaller initiation life and a larger propagation life. Hence, the effect of increase in stress amplitude and duration of exposure is compensated by a smaller critical pit size.

Table 4 shows that the inverse-mapping approach is able to fairly approximate the physical process of corrosion fatigue for most of the cases studied. To get more data, a few test cases were run, where the value of a particular fatigue life (either initiation life or propagation life) or both is maximized. The most desirable condition would be to maximize both portions of the total fatigue life. However, to determine which variables influence the different portions of the fatigue life test cases were run, where all of the damage parameters were allowed to be adjusted, to achieve the desired combinations of fatigue lives. The desired values of the fatigue lives were chosen such that they fall in the experimentally observed range of fatigue lives.

Table 5 shows the different damage parameters predicted by the inverse-mapping network in order for the panels to have only initiation life, only propagation life, or maximum of both the portions. For example, the first simulation (case 1) predicts the damage parameters for no crack initiation life and a propagation life of 398,107 cycles. For case 2 the panel has maximum initiation life and negligibly small propagation life. Similarly, for case 3 the damage parameters are predicted so that a panel has almost no fatigue life, which implies that the pit grows into a crack and causes a failure within a few cycles ($N_i = 4$, $N_p = 73$). The last simulation (case 5) predicts the parameters causing the aluminum panel to have the maximum number of initiation and propagation life cycles (1.95×10^6 and 1.64×10^6 cycles, respectively). The stress amplitude predicted for this case is almost zero, which means that the case is practically a static loading case with small vibrations and negligible load, rather than a fatigue loading case. It is obvious that with these parameters the structure is likely to have a large fatigue life. The initial pit size a_0 for this case is small (5.02×10^{-7} mm), and the critical crack size is relatively large, implying that it will take more cycles to form a crack, and hence the panel will have a higher initiation life. Similarly, the final crack size is also large, which means that the propagation life will also be higher.

Relative Importance of Parameters for Corrosion Fatigue

The parameters affecting the corrosion-fatigue mechanism were also rank ordered according to their relative importance using the procedure described in Sec. III. The results are tabulated in Table 6. It can be observed that the duration of exposure to corrosive environment is the most important parameter for the initiation life, and the critical pit size is the most important parameter for the propagation life. The other four most important parameters for the crack initiation life are stress amplitude, stress ratio, initial pit size, and the critical pit size. The results correctly show the importance of the damage parameters because the critical pit size and the initial pit size affect propagation life more than the initiation life. It can also however be seen that duration of exposure and stress amplitude play more important roles than the initial and critical pit size.

V. Conclusions

The damage parameters corresponding to desired reliability characteristics were predicted using the inverse-mapping approach for two trained neural networks. The damage parameters predicted through the inverse-mapping procedure for both the residual strength and corrosion rate network and corrosion-fatigue network are found to agree well with the experimental data, thus demonstrating the feasibility of the approach. In addition, the damage parameters were also rated according to their relative importance for the fatigue lives, corrosion rate, and residual strength. The results are fairly reasonable. This idea of relative importance can become an important tool for guiding the maintenance engineer to focus attention on particular damage parameters in order to have reliable structure. For example, if a maintenance engineer detects an MSD crack of a particular size in the structure he/she can use the present method to obtain the other damage parameters, say, the lead crack length so that the structure has strength not less than a particular value, and take preventive measures to arrest the lead crack. The desired strength value can be governed by the airworthiness requirements. The results obtained for corrosion fatigue should give a good understanding about the effects of the damage parameters on the initiation and propagation fatigue lives, thereby providing useful information for maintenance and redesign of aircraft structures.

In general, the present approach of estimating the operating environment parameters can be used for the structural redesign/maintenance of aging aircraft structures. Using these models, the maintenance engineer will learn about the maximum extent of damage that can be allowed on the structure so that the structure is still airworthy/operable. To make the present approach into a useful and practical tool for structural integrity redesign, much more work has to be done in terms of additional tests and extend to other damage mechanisms than those considered in the paper.

Acknowledgment

The authors thank the National Science Foundation for funding this research through Grant CMS-9812723.

References

[1] Bartelds, G., "Aircraft Structural Health Monitoring, Prospects for Smart Solutions from a European Viewpoint," *Journal of Intelligent Material Systems and Structures*, Vol. 9, No. 11, 1998, pp. 906–910.

[2] Pidaparti, R. M., Jayanti, S., and Palakal, M. J., "Residual Strength and Corrosion Prediction of Aging Aircraft Panels: A Neural Network Study," *Journal of Aircraft*, Vol. 39, No. 1, 2002, pp. 175–180.

[3]Pidaparti, R. M., Jayanti, S., Sowers, C. A., and Palakal, M. J., "Classification, Distribution, and Fatigue Life of Pitting Corrosion for Aircraft Materials," *Journal of Aircraft*, Vol. 39, No. 3, 2002, pp. 486–492.

[4]Davis, D. T., Chen, Z., Tsang, L., Hwang, J. N., and Chang, A. T. C., "Retrieval of Snow Parameters by Iterative Inversion of a Neural Network," *IEEE Transactions on Geoscience and Remote Sensing*, Vol. 31, No. 4, 1993, pp. 842–852.

[5]DeMers, D., and Kreutz-Delgado, K., "Canonical Parameterization of Excess Motor Degrees of Freedom with Self Organizing Maps," *IEEE Transactions on Neural Networks*, Vol. 7, 1996, pp. 43–55.

[6]DeMers, D., and Kreutz-Delgado, K., "Inverse Kinematics of Dexterous Manipulators," Neural Systems for Robotics, edited by O. Omvidar and P. van der Smagt, Academic Press, New York, 1997, pp. 75–116.

[7]Luzar, J., "Pre-Corroded Fastener Hole Multiple Site Damage Testing," Boeing Co., EA 96-135 TH-041, KC-135 Fleet Support Contract, F34601-96-C-0111, Sept. 1998, pp. 1–46.

[8]Moukawsher, E. J., Heinemann, M. B., and Grandt, A. F., Jr., "Residual Strength of Panels with Multiple Site Damage," *Journal of Aircraft*, Vol. 33, No. 5, 1996, pp. 1014–1021.

[9]Dowling, N. E., *Mechanical Behavior of Materials*, Prentice–Hall, Upper Saddle River, NJ, 1993.

S. Saigal
Associate Editor